



# Design and Simulation of Grid-Connected Photovoltaic Single-Phase Inverters

Gabriel Roméo Tobajio Haoudou<sup>1</sup>, Arnaud Biyobo Obono<sup>2</sup>, Léandre Nneme Nneme<sup>3</sup>, Jean Mbihi<sup>4</sup>

<sup>1</sup> Research Laboratory of Computer Science Engineering and Automation, University of Douala, PB: 1872 Douala, Cameroon, rtobajio@yahoo.fr

<sup>2</sup> Research Laboratory of Computer Science Engineering and Automation, University of Douala, PB: 1872 Douala, Cameroon, obonobiyo@yahoo.fr

<sup>3</sup> Research Laboratory of Computer Science Engineering and Automation, University of Douala, PB: 1872 Douala, Cameroon, leandren@gmail.com

<sup>4</sup> Research Laboratory of Computer Science Engineering and Automation, University of Douala, PB: 1872 Douala, Cameroon, mbihidr@yahoo.fr

Received Date: September 5, 2022 Accepted Date: September 26, 2022 Published Date : October 07, 2022

## ABSTRACT

This paper focuses on a new control strategy for single-phase photovoltaic inverters connected to the electrical power distribution network. The inverter studied is single-phase H bridge, equipped with a robust control strategy by sinusoidal duty cycle modulation.

This new control strategy offers the advantage over the control strategy. Most used control in its first approximation (PWM control technique): A low Hardware complexity; a variable modulation frequency/period; a topology of modulation with feedback. This inverter structure is further composed of the robust PI controllers, a boost chopper and an LCL filter. The low voltage electrical network to which this inverter is connected is materialized and simulated by a voltage source of characteristics 230V-15A-50Hz and synchronized to the latter by a phase-locked loop (PLL). In this article, the main components of the grid-connected PV power plant are modeled and simulated under Matlab/Simulink as well as the simulation of the global behavior of the entire network+PV inverter and the results obtained are presented.

**Key words:** Photovoltaic inverter, Sinusoidal duty cycle modulation, robust controller, PLL, Virtual simulation

## 1. INTRODUCTION

In recent decades, the global challenge has been to develop renewable energy sources, including solar, wind, hydro, etc. These sources are not only free and inexhaustible, but also environmentally benign. These sources are not only free and inexhaustible, but also environmentally friendly [1]. Despite the fact that energy production depends on sunshine (which is always variable), the very high cost and the low conversion efficiency, the photovoltaic market is growing at a considerable rate [2]. This growth is leading to the development of low power

[3]. These sources are usually equipped with storage systems, such as accumulators, which make it possible to compensate for the intermittent nature of the production and thus to be able to react promptly and efficiently to demand depending on the time of day. However, the inclusion of many decentralized sources in the grid leads to many problems, the most important of which are grid stability and the quality of the power available at the common connection point [3, 4]. It is then necessary to properly design the inverter serving as the electrical interface from the source to the grid, and especially to optimally select and size its control to ensure a good interconnection to the distribution grid [5]. Although the PWM control technique is generally the most used in the control of these inverters, the new sinusoidal duty cycle modulation control technique, given its advantages [7- 22], also allows us to develop new prototypes of reliable inverters with performances comparable to that driven by pulse width modulation developed [23].

## 2. METHODS AND TOOLS

### 2.1. General structure of the single-phase grid-connected inverter with sinusoidal duty cycle modulation control

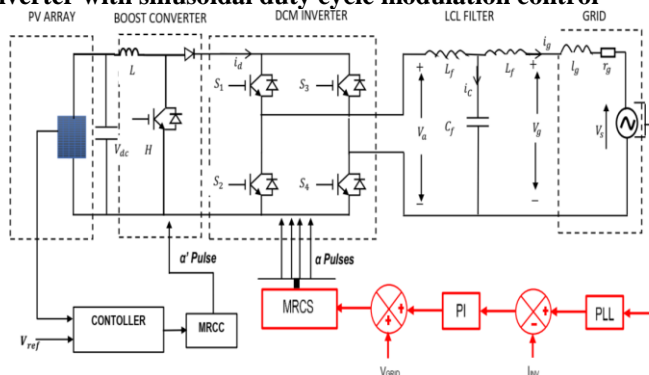


Figure 1: General synoptic

**2.1.1. Photovoltaic panels**

The photovoltaic panels used for the study and simulation are those of 1SOLTECH 1STH-215-P, also having the above characteristics

**Table 1:** PV field parameters

| Elements               | Characteristics             |
|------------------------|-----------------------------|
| PV array               | 10 parallels et 4 series    |
| Irradiance/Temperature | 1000W/m <sup>2</sup> ; 25°C |
| PV current             | 16,50A                      |
| PV voltage             | 182V                        |
| PV power               | 3KW                         |

**2.1.2. Boost chopper**

The structure of the chopper used in this work remains the same as that used in the context of autonomous photovoltaic single-phase inverters with SDCM control and therefore the characteristics are recalled below:  $V_{in}=182V$ ,  $\alpha=0.5$ ,  $V_{out}=364V$ .

**2.1.3. Optimal duty cycle modulator**

The analog power flow model of the duty cycle modulator is given in figure 2 below:

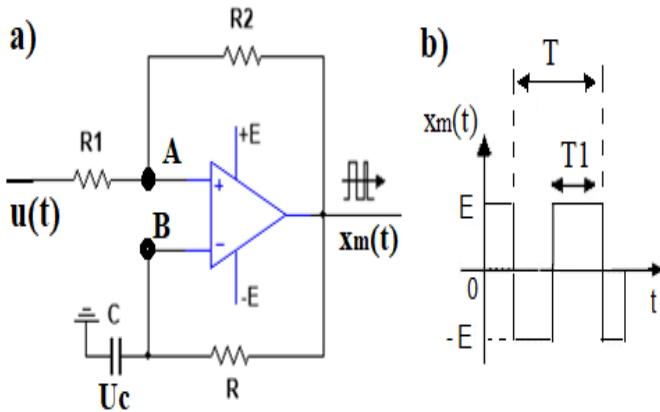


**Figure 2:** Electrical diagram of DCM

Sizing this modulator in duty cycle amounts to determining the values of the passive components R, R<sub>1</sub>, R<sub>2</sub> and C.

These values depend on the base frequency (F<sub>m0</sub>) of the modulator in duty cycle and the latter is obtained by imposing the value of the modulating signal at zero (u=0) in equation (1).

$$T = RC \ln \left[ \frac{\left(2 \frac{R_1}{R_2} + 1\right)^2 - \left(\frac{u}{E}\right)^2}{1 - \left(\frac{u}{E}\right)^2} \right] \quad (1)$$

$$F_{m0} = \frac{1}{T_0}$$

$$F_{m0} = \frac{1}{2RC \ln \left(2 \frac{R_1}{R_2} + 1\right)} \quad (2)$$

This sizing approach allows obtaining the parameters of the modulator in duty cycle but with a wide range of trial and error, hence the welcome of an optimization algorithm of the parameters of the modulator in duty cycle synthesized by equation (3) [2].

$$\alpha^* = \text{Max}_\alpha \left( p_m(\alpha) = \frac{\alpha}{E(1+\alpha) \ln \left(\frac{1+\alpha}{1-\alpha}\right)} \right)$$

with

$$f_{m0}(\alpha) = \frac{1}{2\tau \ln \left(\frac{1+\alpha}{1-\alpha}\right)} \quad (3)$$

$$f_{\min}(u_{\max}, \alpha) = \frac{1}{\tau \ln \left( \frac{((1-\alpha)u_{\max})^2 - ((1-\alpha)E)^2}{((1-\alpha)u_{\max})^2 - ((\alpha-1)E)^2} \right)}$$

$0 < \alpha < 1$

The optimal parameters obtained and presented in Table 2 below of the duty cycle modulator, were determined with the fmincom optimization tool from matlab in accordance with the cost function stated in equation (3).

**Table 2:** Optimal duty cycle modulator settings

|                      | Elements used   | Simulation parameters   | Electronic parameters  |
|----------------------|---|---|--|
| Duty cycle modulator | $f_{m0} = 1 \text{ Mhz}$<br>$E = 5V$<br>$X_{\max} = 4V$ | $\alpha = 0.8571428571428571$<br>57<br>$\alpha_2 = 1 - \alpha = 0.14285714285714285$<br>$\tau = RC = 1.7380297483 \cdot 10^{-06}$ | $R = 1.5k\Omega$ ;<br>$C = 1.1587nF$<br>$R_1 = 10k\Omega$ ;<br>$R_2 = 60k\Omega$<br>Slew rate = 1000V/us |

**2.1.4. Phase Locked Loop (PLL)**

In order to synchronize the output current of the inverter with the grid voltage in order to give a clean sinusoidal current reference, a classic PLL is used for this purpose and therefore the structure is shown in Figure 3 below:

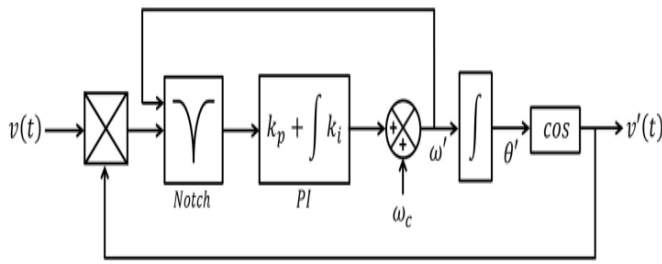


Figure 3: Structure of the PLL used

The model in the form of a block diagram is then presented in Figure 4.

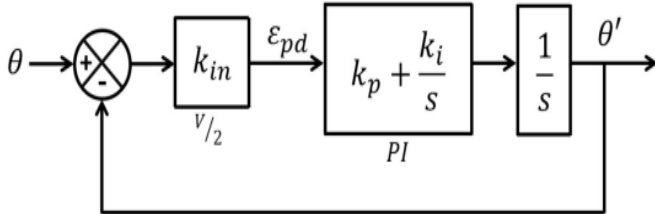


Figure 4: Block diagram of the linearized system

This functional diagram is translated into a transfer function and given by the standard form:

$$H_{PPL}(s) = \frac{2\xi\omega_n \cdot s + \omega_n^2}{s^2 + 2\xi\omega_n \cdot s + \omega_n^2} \quad (4)$$

with

$$\begin{cases} k_p = \frac{2\xi\omega_n}{k_{in}} \\ k_i = \frac{\omega_n^2}{k_{in}} \end{cases} \text{ or } \begin{cases} \xi = \frac{k_{in}k_p}{2\sqrt{k_{in}k_i}} \\ \omega_n = \sqrt{k_{in}k_i} \end{cases} \quad (5)$$

Table 3: Table of values

| f <sub>min</sub> (Hz) | f <sub>c</sub> (Hz) | f(Hz) | K <sub>P</sub> | K <sub>I</sub> |
|-----------------------|---------------------|-------|----------------|----------------|
| 45                    | 25                  | 50    | 180            | 3200           |

### 2.1.5. LCL harmonic filter

Its important in filtering the switching frequency and the surrounding frequencies. The rectangular voltage at the output of the bridge corresponds to the voltage  $v_a$ , while  $v_s$  is the voltage at the output of the total system, connected to the PCC. The best alternative is the LCL filter. The LCL third-order low-pass filter, placed at the output of the bridge, offers good attenuation even with low values of  $L_{1,2}$  and  $C$ , as well as low output current ripple despite its complex structure.

#### 2.1.5.1. Frequency analysis of the LCL filter

The open loop transfer function of the LCL filter in Laplace space is written:

$$F_{LCL}(p)|_{V_s=0} = \frac{I_g(p)}{V_a(p)} = \frac{Z_C}{Z_C(Z_{L1} + Z_{L2}) + Z_{L1}Z_{L2}} \quad (6)$$

By replacing the different elements by their expression in Laplace's symbolic space, we obtain equation 7.

$$F_{LCL}(p)|_{V_s=0} = \frac{1}{p(L_1 + L_2) + p^3(C \cdot L_1 \cdot L_2)} \quad (7)$$

The frequency analysis of this transfer function leads us to the Bode diagram, whose amplitude and phase are given in figure 5 below:

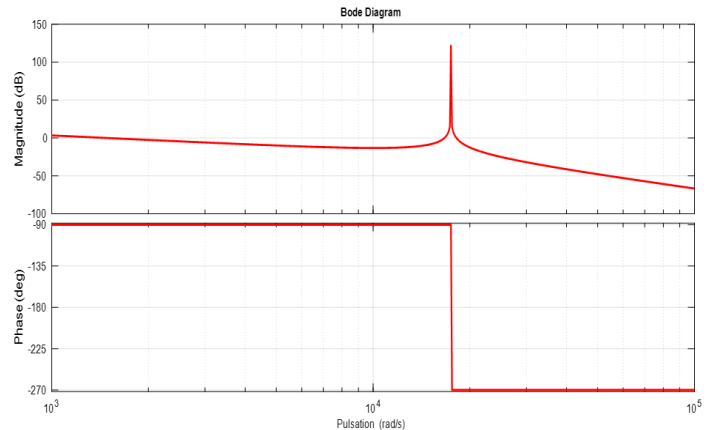


Figure 5: Bode Diagram in BO of the system

#### 2.1.5.2. Characterization of the output filter

In order to avoid resonance and instability problems, it is recommended to maintain this resonance frequency between 10 times the line frequency (50Hz), and half the switching frequency of the inverter:

$$F_{rés,LCL} \in \left[ 10f_s, \frac{f_d}{2} \right] \Rightarrow F_{rés,LC} \in [0.5 ; 12.5] \text{ kHz} \quad (8)$$

Its resonant frequency is given by:

$$F_{rés,LCL} = \frac{1}{2\pi} \sqrt{\frac{L_1 + L_2}{C \cdot L_1 \cdot L_2}} \text{ AN: } F_{rés,LCL} = 2.77 \text{ kHz} \in [0.5 ; 12.5] \text{ kHz} \quad (9)$$

Table 4: Table of values

| Elements   | Characteristics |
|------------|-----------------|
| $L_1, r$   | 700μH, 1mΩ      |
| $L_2, r$   | 200μH, 1mΩ      |
| $C, r$     | 42μH, 1mΩ       |
| $F_{reso}$ | 812 kHz         |

#### 2.1.5.3. Closed loop stability

The Bode Rivers Criterion therefore applied to the asymptotic Bode diagram of Figure 5 leads to the conclusion that the closed-loop system is unstable. Hence the need for a control law for stabilizing the current/voltage quantities at the common connection point.

### 3. RESULTS OBTAINED AND DISCUSSIONS

#### 3.1. Virtual simulation platform and structure

Matlab's Simulink environment is the platform used to perform the virtual simulations on the inverter prototype presented in this work [24].

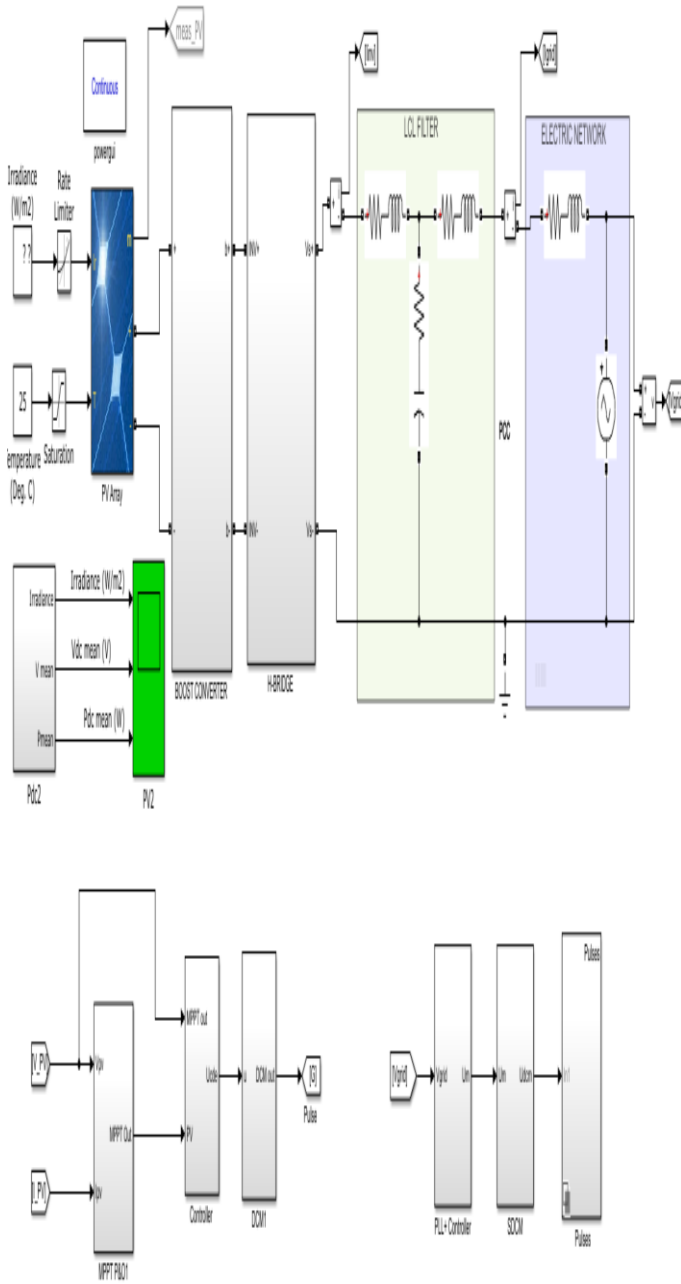


**Figure 5:** Simulink structure of the autonomous PV inverter with DCM control

#### 3.2. Results of simulations and discussions

##### 3.2.1. Current and voltage at the output of the PV array

The current and voltage characteristics as a function of time at the output of the photovoltaic field are those of figure 6 below. It

can be seen that the PV array delivers a constant current of 16.5A under a constant DC voltage of 182V.

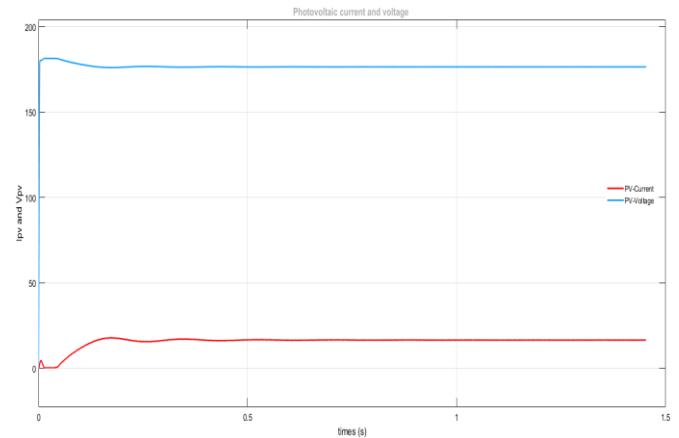


**Figure 6:** PV array current and voltage

##### 3.2.2. Voltage at the output of the boost chopper

The voltage at the input of the bridge is 364V, corresponding to a voltage at the input of the BOOST chopper of 182V under a duty cycle  $\alpha=0.5$ . We clearly see in the figure below that the output voltage of the parallel chopper increases and stabilizes at the output value of 364V.

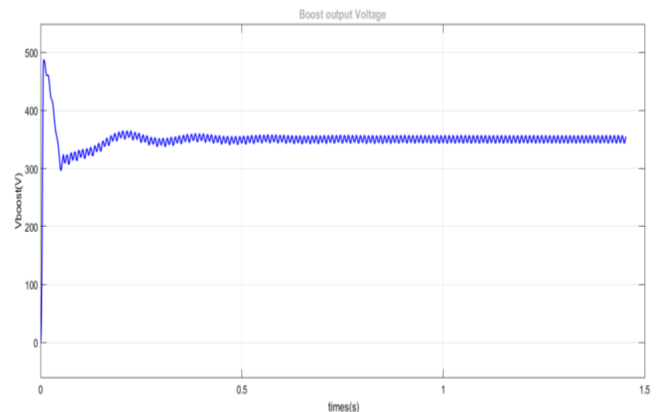


**Figure 6:** Voltage at the output of the boost chopper

##### 3.2.3. Voltage and current at the output of the inverter

Are respectively given in blue and red in Figure 7, the voltage and the current at the output of the H-bridge.

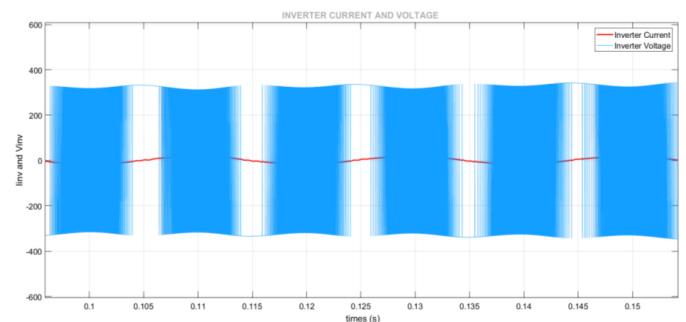


**Figure 7:** Voltage and current at the output of the inverter

**3.2.4. Harmonic spectrum of the voltage at the output of the inverter**

Figure 8 below shows the evolution of the harmonics in the steady state signal. We can see that the harmonic distortion rate is very disastrous, that is to say an overall rate of THD = 106.91%.

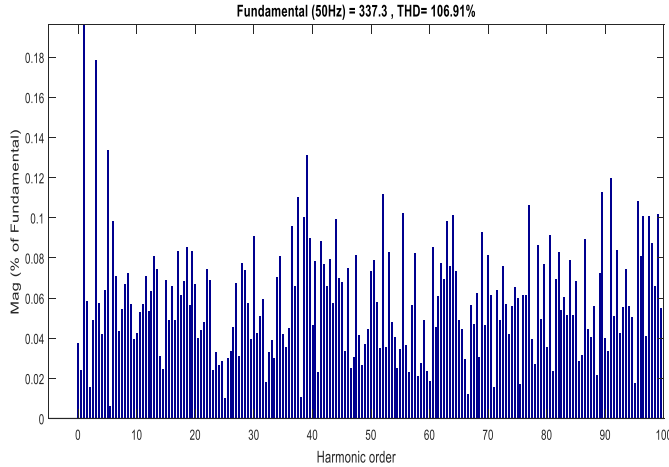


**Figure 8:** Harmonic spectrum of the voltage at the output of the inverter

**3.2.5. Harmonic spectrum of the current at the output of the PV inverter**

It can be seen that the overall current harmonic distortion rate at the output of the inverter is 10.76%. THD not acceptable according to the EN50160 standard.

**Figure 9:** Harmonic spectrum of the current at the output of the inverter

**3.2.6. Mains voltage and current**

The electrical network is modeled and simulated by a source of characteristics:  $V_{res}=230V$ ,  $I_{res}=14A$ ,  $f=50Hz$

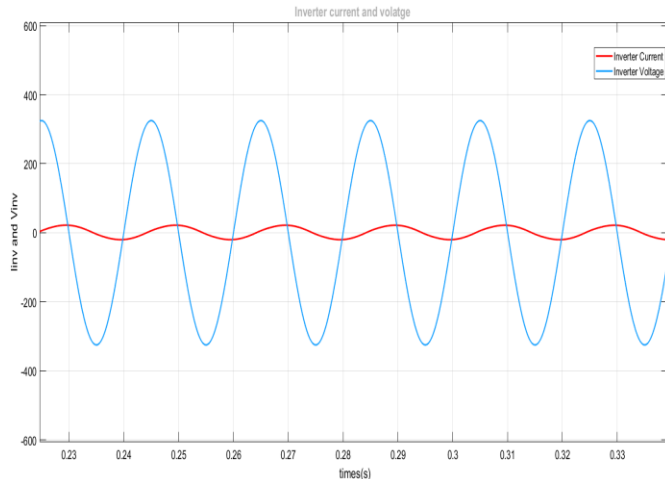


**Figure 10:** Voltage at common connection points

**3.2.7. Evolution of the source voltage harmonic distortion rate**

It can be seen that outside the system start-up phase, the overall voltage harmonic distortion rate is 0.00%. THD acceptable according to standard EN50160

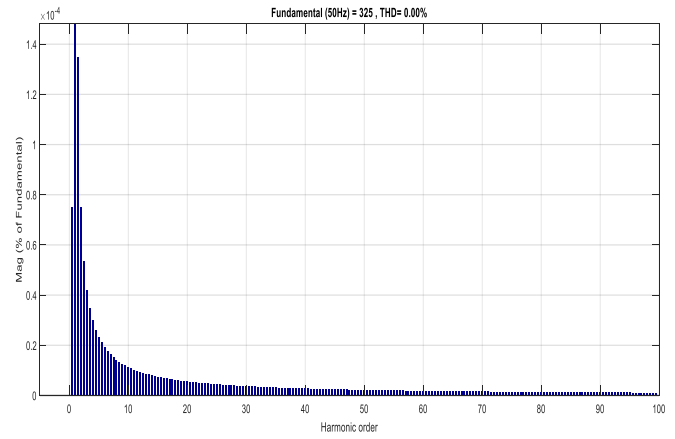


**Figure 11:** Harmonic spectrum of the voltage at the common connection points

**3.2.8. Current harmonic distortion rate**

It can be seen that the source current harmonic distortion rate is 2.07%. THD acceptable according to standard EN50160.

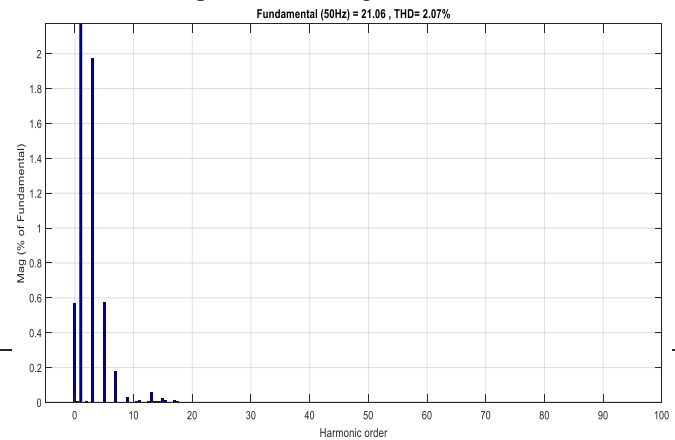


**Figure 12:** Harmonic spectrum of current at the common connection points

**4. CONCLUSION**

This study presents a new principle of control of single-phase PV inverters connected to the electrical distribution network using a phase-locked loop. The inverter structure, whose originality is essentially based on its control strategy (control by modulation in duty cycle) and equipped with an LCL output filter, presents an inexpensive and easy-to-monitor architecture. It also allows simple and quick maintenance. The general structure, modeling and simulation of the grid-connected PV inverter are presented as well as the virtual simulation results in the Matlab/Simulink platform.

**REFERENCES**

[1] Renewables 2014. Global Status Report, Paris, Renewable Energy Policy Network for the 21st Century, s.d., p. 21 et s.  
 [2] Bao, C., Ruan, X., Wang, X., Li, W., Pan, D., & Weng, K. (2013). Step-by-Step Controller Design for LCL-Type Grid-Connected Inverter with Capacitor-Current-Feedback Active-

- Damping. IEEE Transactions on Power Electronics, 29(3), 1239-1253.
- [3] Atiqah Hamizah Mohd Nordin, Ahmad Maliki Omar, Hedzlin Zainuddin « Modeling and Simulation of Grid Inverter in GridConnected Photovoltaic » system international journal of renewable energy research ,Vol. 4, No. 4, 2014.
- [4] Sachin Jain and Vivek Agarwal, , « A Single-Stage Grid Connected Inverter Topology for Solar PV Systems With Maximum Power Point Tracking » IEEE transactions on power electronics, vol. 22, no. 5, september 2007
- [5] Soeren Baekhoej Kjaer, John K. Pedersen, and Frede Blaabjerg, « A Review of Single-Phase Grid-Connected Inverters for Photovoltaic Modules » IEEE transactions on industry applications, vol. 41, no.5, september/october 2005.
- [6] Blaabjerg, F., Teodorescu, R., Liserre, M., & Timbus, A. V. (2006). Overview of Control and Grid Synchronization for Distributed Power Generation Systems. IEEE Transactions on Industrial Electronics, 53(5), 1398-1409
- [7] Jean Mbihi, "Informatique et automation: Automatismes programmables contrôlés par ordinateur", pp. 103-113, EditonsPublibook, 2005.
- [8] J.Mbihi, B. Ndjali, and M. Mbouenda, "Modelling and simulation of a class of duty cycle modulators for industrial instrumentation", Iranian Journal of Electrical and Computer Engineering, vol.4, N°2, pp. 121-128, 2005.
- [9] J. Mbihi, F. Ndjali Beng, M. Kom, and L. NnemeNneme, "A novel analog-to-digital conversion technique using nonlinear duty-cycle modulation", International Journal of Electronics and Computer Science Engineering, Volume 1, Number 3, pp. 818-825, 2012.
- [10] J. Mbihi, L. NnemeNneme, "A multi-channel analog-to-digital conversion technique using parallel duty-cycle modulation", International Journal of Electronics and Computer Science Engineering, Volume 1, Number 3, pp. 826-833, 2012.
- [11] B. MoffoLonla, J. Mbihi, L. Nneme Nneme, and M. Kom, "A novel digital-to-analog Conversion technique using duty-cycle modulation", International Journal of Circuits, Systems and Signal Processing, Issue 1, Vol. 7, pp. 42-49, 2013
- [12] B. MoffoLonla, J. Mbihi, L. NnemeNneme, and M. Kom, "A Low Cost and High Quality Duty-Cycle Modulation Scheme and Applications", International Journal of Electrical, Computer, Energetic, Electronic and Communication Engineering Vol:8, No:3, 2014.
- [13] L. N. Nneme, B. M. Lonlaand J. Mbihi « Review of a Multipurpose Duty-Cycle ModulationTechnology in Electrical and Electronics Engineering », p. 10.
- [14] J. Mbihi, L. NnemeNneme "virtual simulation and comparison of sine pulse zidhand sine duty cycle modulation drivers for single phase power inverters", JEEECCS, Volume 6, Issue 21, pages 31-38, 2020.
- [15] M.J.P. Pesdjock, J.R.M. Pone, D.Tchiotsop, M.R. Douanla, G. Kenne "minimization of currents harmonics injected for grid connected photovoltaic system using duty cycle modulation technique", International Journal of dynamic and control, 31 October 2020.
- [16] A. O. Biyobo, L. N. Nneme, et J. Mbihi, « A Novel Sine Duty-Cycle Modulation Control Scheme for Photovoltaic Single-Phase Power Inverters », vol. 17, p. 9, 2018.
- [17] P. O. Etouke, L. N. Nneme, J. Mbihi « An Optimal Control Scheme for a Class of Duty-Cycle Modulation Buck Choppers: Analog Design and Virtual Simulation », Journal of Electrical Engineering, Electronics, Control and Computer Science –JEEECCS, Volume 6, Issue 19, pages 13-20, 2020
- [18] Y. P. DangweSounsoumo, Jean Mbihi, Haman-djalo and Joseph Yves Effa, "Virtual Digital Control Scheme for a Duty-Cycle Modulation BoostConverter ", Journal of Computer Science and Control Systems, Volume 10, No 2, pp. 22-27, October 2017, Romania.
- [19] Y. P. DangweSounsoumo, HamanDJALO, Jean Mbihi et J. Y. EFFA , " Modélisation et simulation virtuelle d'un nouveau schéma de réglage de hacheurs Boost à commande rapprochée par modulation en rapport cyclique ", Journal Afrique Science , pp. 176-185, Vol. 13, No. 1, 2017, Côte d'Ivoire, <http://www.afriquescience.info>.
- [20] J. Mbihi, L. NnemeNneme, "A novel Control Scheme for Buck Power Converters using Duty-Cycle Modulation", International Journal of Power Electronics, Vol. 5, N°3/4, pp 185 - 199, October 2013, Switzerland..
- [21] Nguefack Tatou Laurel, Paune Felix, Kenfack W. Gutenberg, Mbihi Jean «A Novel Optical Fiber Transmission System Using Duty-Cycle Modulation and Application to ECG Signal: Analog Design and Simulation » Journal of Electrical Engineering, Electronics, Control and Computer Science – JEEECCS, Volume 6, Issue 21, pages 39-48, 2020.
- [22] Otam Steve Ulriche, MoffoLonla Bertrand, GamomNgounou E. R. Christian, Mbihi Jean « A novel FPGA-Based Multi-Channel Signal Acquisition System Using Parallel Duty-Cycle Modulation and Application to BiologicSignals: Design and Simulation » Journal of Electrical Engineering, Electronics, Control and Computer Science –JEEECCS, Volume 7, Issue 24, pages 13-20, 2021
- [23] G.R Tobajio Haoudou, A. Biyobo Obono, Léandre .N. Nneme « Design and Simulation of a New Topology of Single-Phase Stand-Alone Solar Inverters by Sinusoidal Duty Cycle Modulation » International Journal of Scientific Research and Engineering Development—IJSRED, Volume 5, Issue 2, pages 154-161, 2022
- [24] L. O. Aghenta and M. Tariq Iqbal « Design and Dynamic Modelling of a Hybrid Power System for a House in Nigeria » International Journal of Photoenergy, Volume 2019.